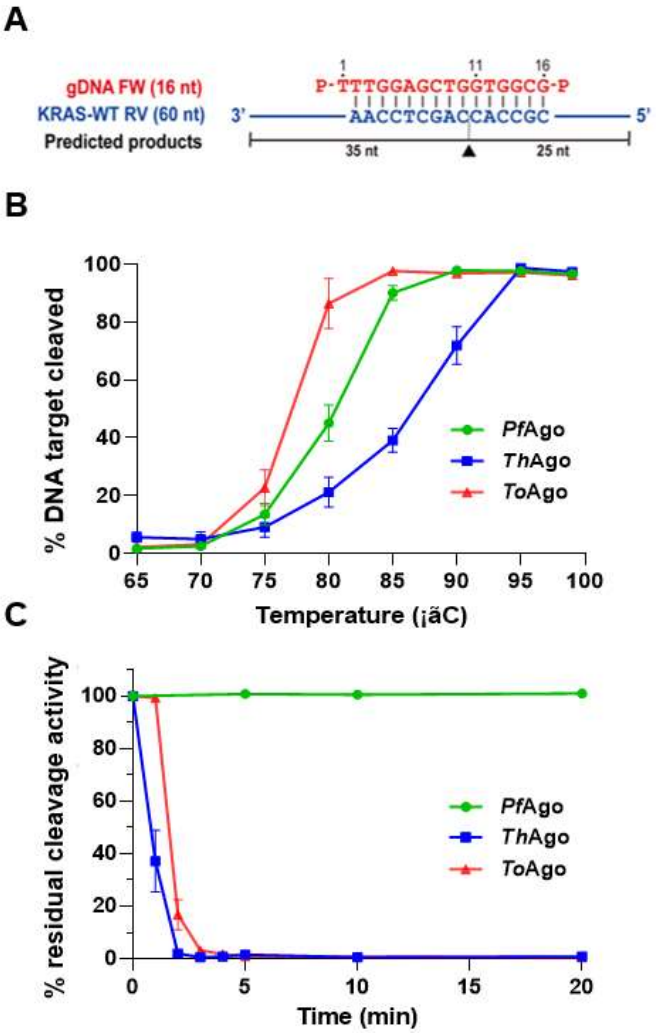

Figure S1. Evaluation of the temperature dependence and thermostability of hyperthermophilic Agos cleavage activity on the ssDNA target. **(A)** Sequences of the ssDNA target and gDNA. **(B)** Effect of temperature on ssDNA cleavage efficiency. *Pf*Ago, *Th*Ago and *To*Ago was incubated with a 16 nt gDNA and 60 nt ssDNA of *KRAS* G12D as a target at a 1:10:1 molar ratio (Ago: gDNA: tDNA) at various temperatures for 15 min with 0.5 mM Mn^{2+}, respectively. **(C)** Effect of thermostability on ssDNA cleavage efficiency. *Pf*Ago, *Th*Ago and *To*Ago was incubated with a 16 nt gDNA and 60 nt ssDNA of *KRAS* G12D as a target at a 1:10:1 molar ratio (Ago: gDNA: tDNA) at 95 ℃ for various reaction time with 0.5 mM Mn^{2+}, respectively. The cleavage products were resolved in denaturing polyacrylamide gels. *Th*Ago: *Thermococcus thioreducens* Argonaute (NCBI accession no. WP_055429304.1); *To*Ago: *Thermococcus onnurineus* Argonaute (NCBI accession no. WP_012572468.1); M: ssDNA Marker; nt: nucleotides.

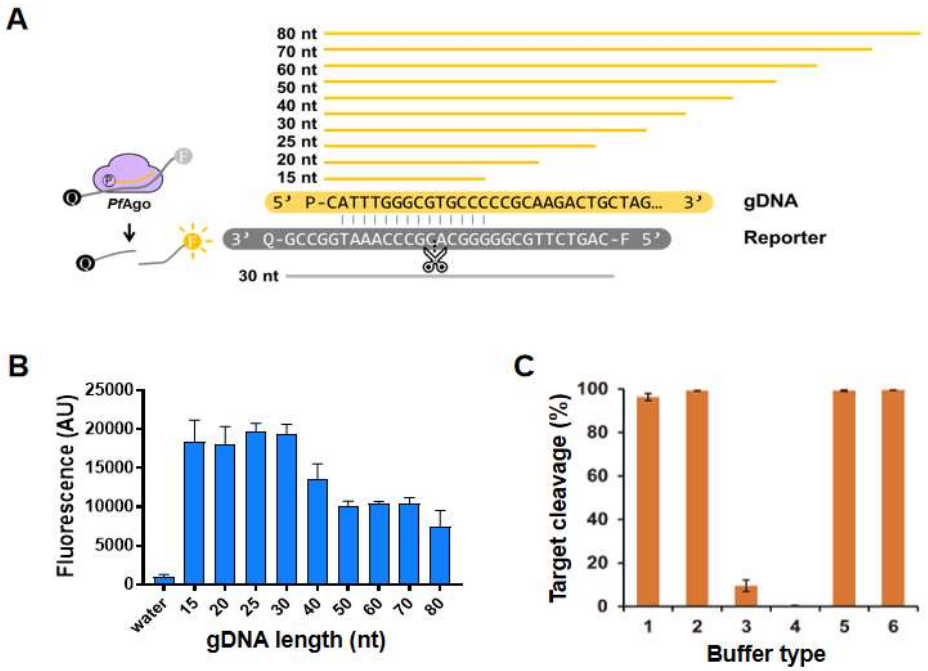

Figure S2. Effects of gDNA length and buffer component on cleavage efficiency. **(A)** Schematic of overlapping sequence between gDNA and the fluorophore-labelled ssDNA target. **(B)** Fluorophore-labelled ssDNA cleavage was catalyzed by gDNA-mediated *Pf*Ago of different lengths. The fluorescence signal was measured from the cleavage product of fluorophore-labelled ssDNA after 15 min at 95 °C. **(C)** The ssDNA cleavage in various PCR buffers. *Pf*Ago was incubated with 16-nt gDNAs and 60 nt of ssDNA targets at a 1:10:1 molar ratio (*Pf*Ago: gDNA: tDNA) at 95 °C for 15 min. Buffer 1: 1×Reaction Buffer; Buffer 2: abm 2×PCR Taq Master Mix; Buffer 3: abm 2×PCR PrecisionTM Master Mix; Buffer 4: TaKaRa PrimeSTAR Max Premix (2×); Buffer 5: AG 2×Pro Taq HS Probe Premix; Buffer 6: Vazyme 2×AceQ qPCR Probe Master Mix. The cleavage products were resolved in denaturing polyacrylamide gels. Histogram data were calculated from gels quantitatively analyzed by Quantity One software. Error bars represent the s.d. of the means (n = 3).

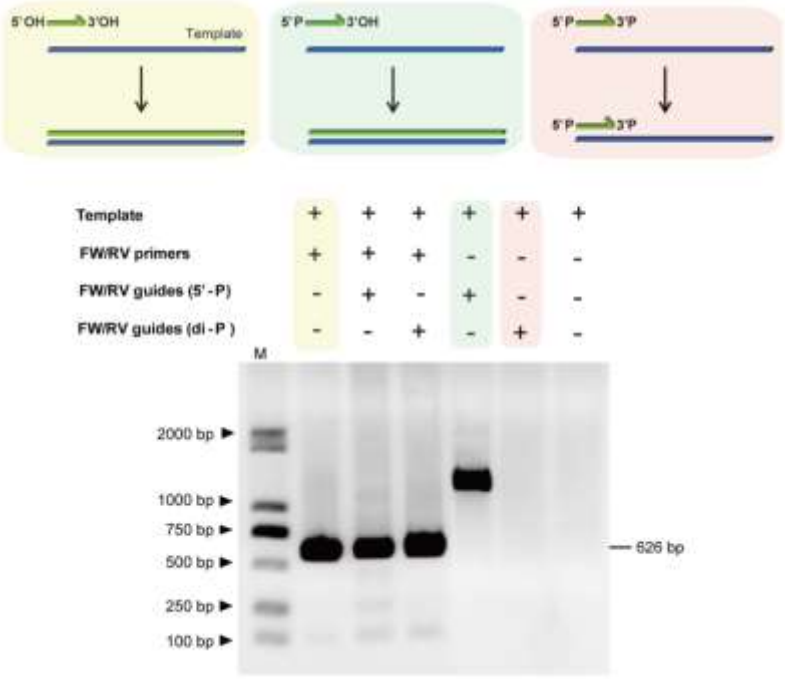

Figure S3. Evaluation of the di-phosphate gDNA dependence of *Pf*Ago cleavage activity on the ssDNA target. A plasmid containing *KRAS* G12D as the template was used for PCR. A pair of primers was designed for the 626 bp of the *KRAS* G12D amplicon, and a pair of gDNAs were designed with either 5'-phosphate (5'-P) or 5', 3'-di-phosphate (di-P) modification across the *KRAS* G12D SNV site. Thermal cycling started with a preincubation step at 94 ℃ for 3 mins for polymerase activation, followed by 30 PCR cycles (94 ℃ for 30 s, 55 ℃ for 30 s, and 72 ℃ for 20 s). The products were resolved using an agarose gel. M: dsDNA Marker; bp: base pairs; 5'-P: only the 5'-terminus is modified by a phosphate group; di-P: both the 5'- and 3'-termini are modified by phosphate groups.

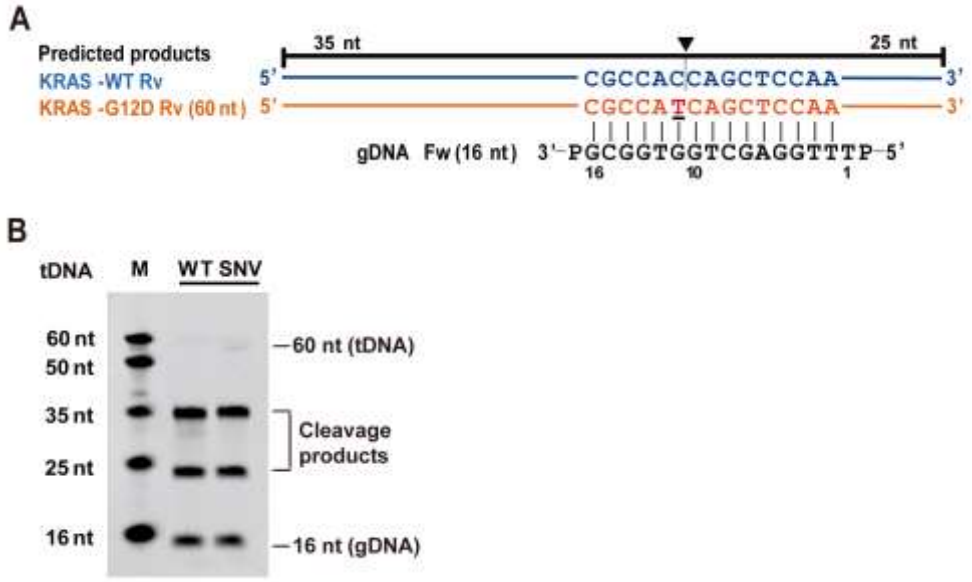

Figure S4. Comparison of cleavage efficiencies of WT and SNV ssDNA targets directed by gDNA complementary to the WT sequence. **(A)** Schematic diagram of the gDNA and ssDNA targets in the reverse strands of *KRAS* G12D WT and SNV. **(B)** Gel electrophoresis of the cleavage products of reverse strands of *KRAS* G12D WT and SNV directed by the corresponding gDNA at varied temperatures. *Pf*Ago was incubated with 16-nt gDNAs and 60 nt of WT or variant ssDNA targets at a 1:10:1 molar ratio (*Pf*Ago: gDNA: tDNA) at 95 °C for 15 min. The cleavage products were resolved in denaturing polyacrylamide gels. M: ssDNA marker; nt: nucleotides.

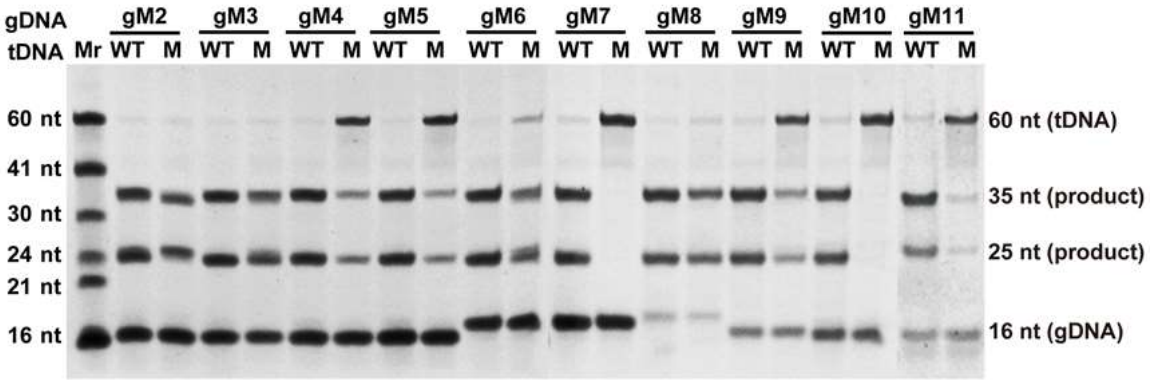

Figure S5. Discriminating cleavage of the *KRAS* G12D ssDNA target using gDNAs with an extra mismatch. Electropherogram of the cleavage products of the *KRAS* G12D WT and SNV ssDNA targets using the designed gDNAs. *Pf*Ago was incubated with 16 nt serial gDNAs containing mismatches from positions 2 to 11, and 60 nt of the WT and variant ssDNAs as targets at a 1:10:1 molar ratio (*Pf*Ago: gDNA: tDNA) at 95 °C for 15 min. The cleavage products were resolved in denaturing polyacrylamide gels. Mr: ssDNA marker; nt: nucleotides.

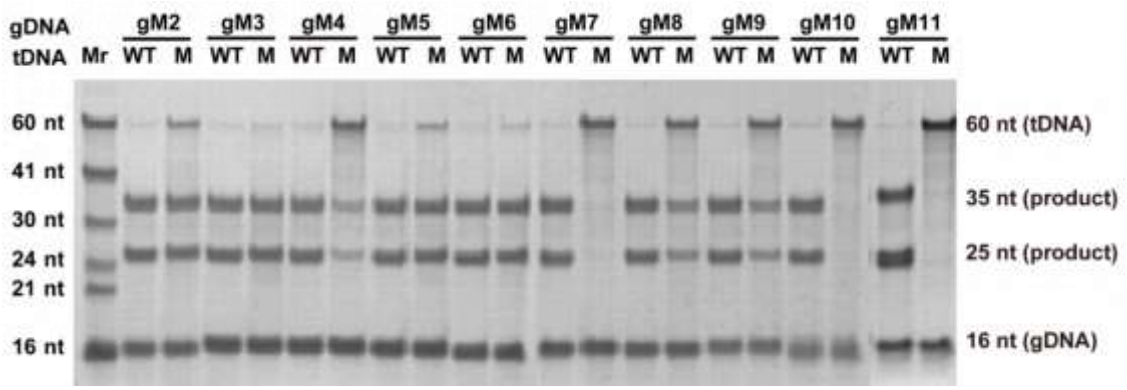

Figure S6. Discriminating cleavage of the *PIK3CA* E545K ssDNA target using gDNAs with an extra mismatch. Electropherogram of the cleavage products of the *PIK3CA* E545K WT and SNV ssDNA targets using the designed gDNAs. *Pf*Ago was incubated with 16 nt serial gDNAs containing mismatches from positions 2 to 11 and 60 nt of the WT and variant ssDNAs as targets at a 1:10:1 molar ratio (*Pf*Ago: gDNA: tDNA) at 95 °C for 15 min. The cleavage products were resolved in denaturing polyacrylamide gels. Mr: ssDNA marker; nt: nucleotides.

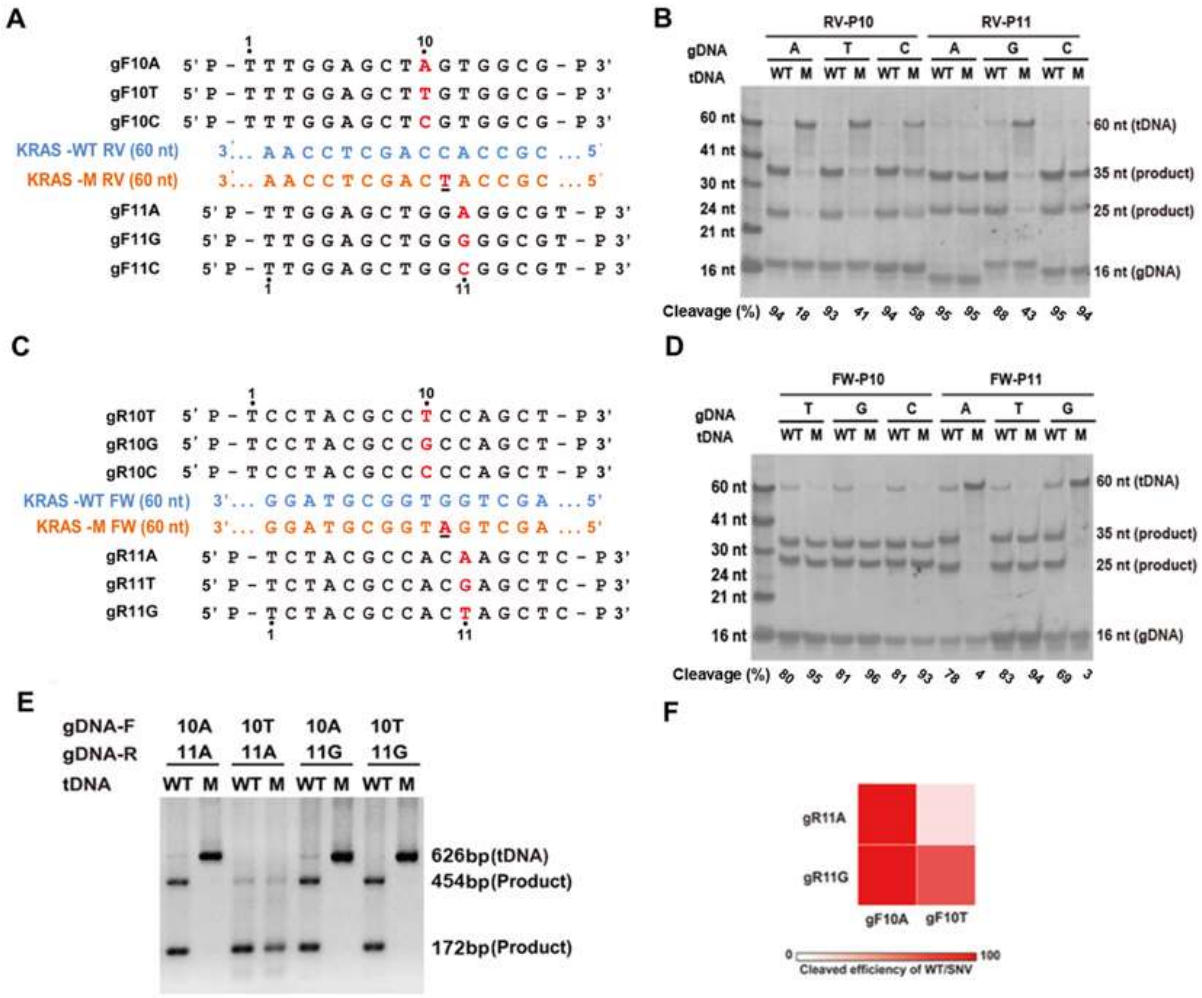

Figure S7. Characterization of the discriminating cleavage of *KRAS* G12D targets directed by synthetic gDNA with nucleotide identity at position 10 or 11. **(A)** and **(C)** show the design of the gDNAs with different nucleotide substitutions at position 10 or 11 for both strands of the ssDNA targets. Mismatches are shown in red with the positions indicated. **(B)** and **(D)** show the results of gel electrophoresis of cleavage products for each strand of the ssDNA targets. **(E)** and **(F)** show the cleavage products for dsDNA targets and the corresponding heatmap of discriminating cleavage activity. *Pf*Ago was incubated with 16 nt gDNAs and the WT and SNV ssDNA or dsDNA targets in a 1:10:1 molar ratio (*Pf*Ago: gDNA: tDNA) at 95 °C for 15 min. The cleavage products were resolved in denaturing polyacrylamide gels **(B, D)** and agarose gels **(E)**. The specificity index in the heatmap is calculated as the ratio of the cleavage efficiency of WT to that of SNV. Mr: ssDNA marker; M: SNV ssDNA or dsDNA target; nt: nucleotides; bp: base pairs.

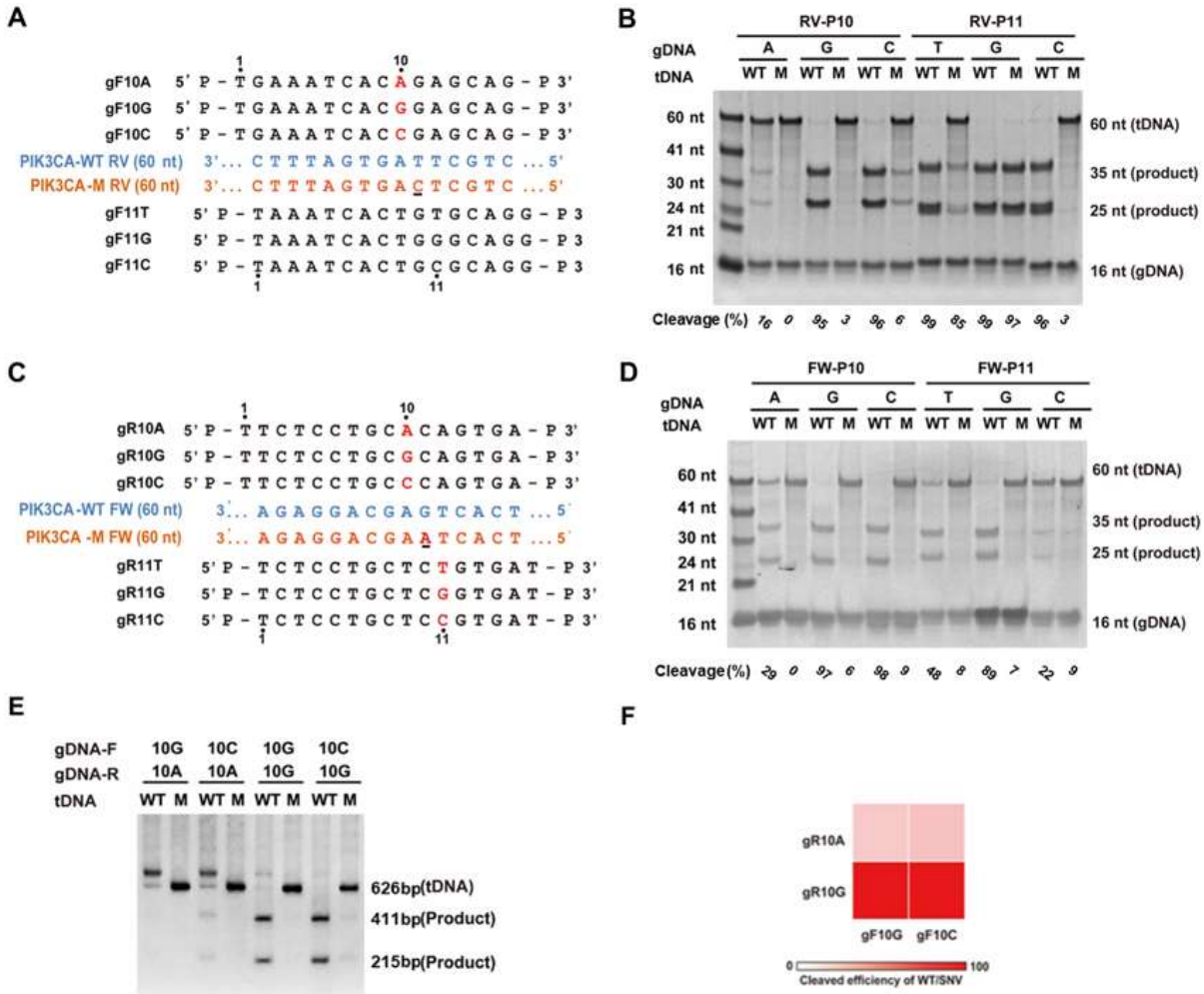

Figure S8. Characterization of the discriminating cleavage of *PIK3CA* E545K targets directed by synthetic gDNA with nucleotide identity at position 10 or 11. **(A)** and **(C)** show the design of gDNAs with different nucleotide substitutions at position 10 or 11 for both strands of the ssDNA targets. Mismatches are shown in red with the positions indicated. **(B)** and **(D)** show the results of gel electrophoresis of the cleavage products for each strand of the ssDNA targets. **(E)** and **(F)** show the cleavage products for dsDNA targets and the corresponding heatmap of discriminating cleavage activity. *Pf*Ago was incubated with 16 nt gDNAs and the WT and SNV ssDNA or dsDNS targets at a 1:10:1 molar ratio (*Pf*Ago: gDNA: tDNA) at 95 °C for 15 min. The cleavage products were resolved in denaturing polyacrylamide gels **(B, D)** and agarose gels **(E)**. The specificity index in the heatmap is calculated as the ratio of the cleavage efficiency of WT to that of SNV. Mr: ssDNA marker; M: SNV ssDNA or dsDNA target; nt: nucleotides; bp: base pairs.

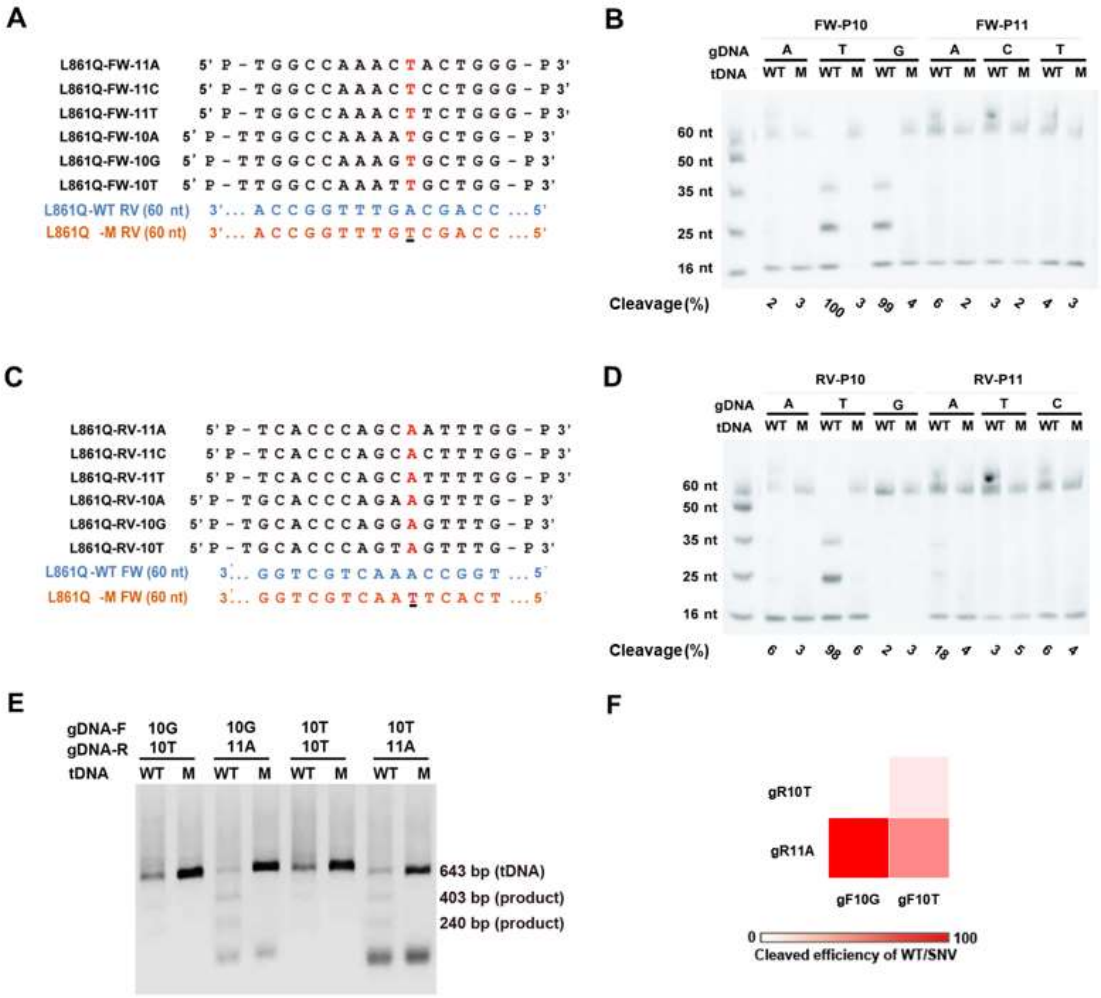

Figure S9. Characterization of the discriminating cleavage of *EGFR* L861Q targets directed by synthetic gDNA with nucleotide identity at position 10 or 11. **(A)** and **(C)** show the design of the gDNAs with different nucleotide substitutions at position 10 or 11 for both strands of the ssDNA targets. Mismatches are shown in red with the positions indicated. **(B)** and **(D)** show the results of gel electrophoresis of cleavage products for each strand of the ssDNA targets. **(E)** and **(F)** show the cleavage products for dsDNA targets and the corresponding heatmap of discriminating cleavage activity. *Pf*Ago was incubated with 16 nt gDNAs and the WT and SNV ssDNA or dsDNA targets in a 1:10:1 molar ratio (*Pf*Ago: gDNA: tDNA) at 95 °C for 15 min. The cleavage products were resolved in denaturing polyacrylamide gels **(B, D)** and agarose gels **(E)**. The specificity index in the heatmap is calculated as the ratio of the cleavage efficiency of WT to that of SNV. Mr: ssDNA marker; M: SNV ssDNA or dsDNA target; nt: nucleotides; bp: base pairs.

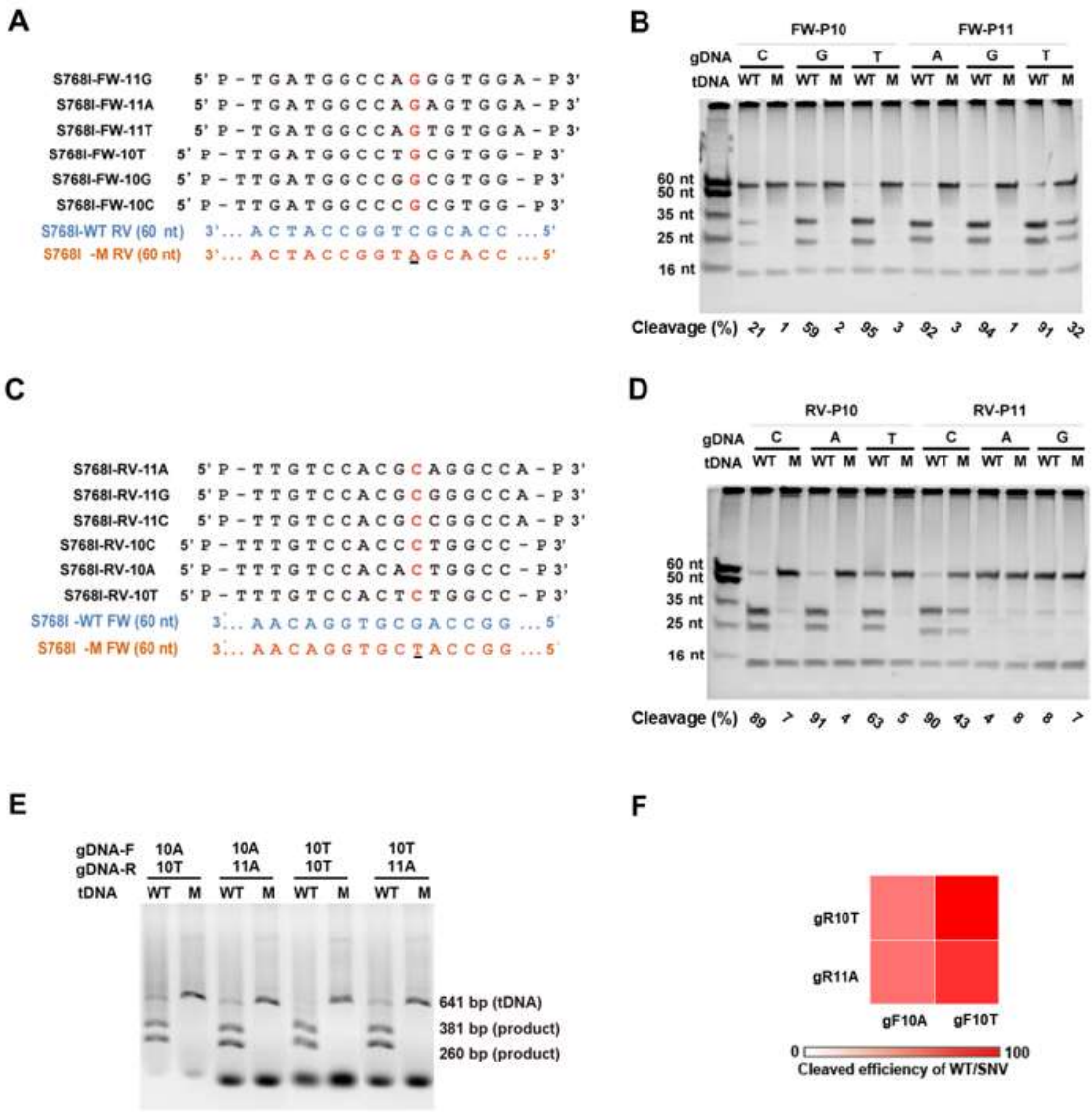

Figure S10. Characterization of the discriminating cleavage of *EGFR* S768I targets directed by synthetic gDNA with nucleotide identity at position 10 or 11. **(A)** and **(C)** show the design of the gDNAs with different nucleotide substitutions at position 10 or 11 for both strands of the ssDNA targets. Mismatches are shown in red with the positions indicated. **(B)** and **(D)** show the results of gel electrophoresis of cleavage products for each strand of the ssDNA targets. **(E)** and **(F)** show the cleavage products for dsDNA targets and the corresponding heatmap of discriminating cleavage activity. *Pf*Ago was incubated with 16 nt gDNAs and the WT and SNV ssDNA or dsDNA targets in a 1:10:1 molar ratio (*Pf*Ago: gDNA: tDNA) at 95 °C for 15 min. The cleavage products were resolved in denaturing polyacrylamide gels **(B, D)** and agarose gels **(E)**. The specificity index in the heatmap is calculated as the ratio of the cleavage efficiency of WT to that of SNV. Mr: ssDNA marker; M: SNV ssDNA or dsDNA target; nt: nucleotides; bp: base pairs.

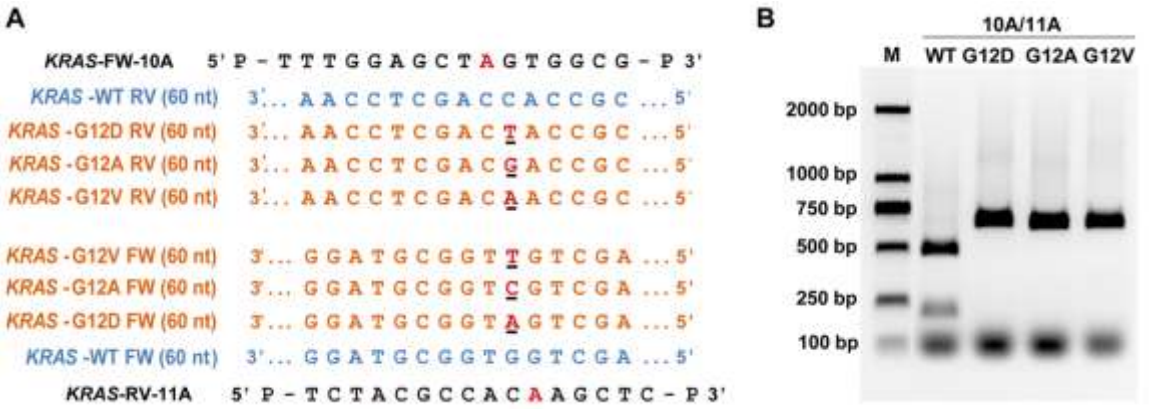

Figure S11. Cleavage discrimination of three *KRAS* SNVs to WT directed by a pair of gDNAs. **(A)** Sequences of designed guides corresponds to *KRAS* WT target and three *KRAS* SNVs. **(B)** Cleavage efficiency of three *KRAS* SNVs and WT directed by a pair of gDNAs. *Pf*Ago loaded with 16-nt gDNAs was incubated with the corresponding DNA target in a 1:10:1 molar ratio (*Pf*Ago: gDNA: tDNA) at 95 °C for 15 min. Nucleic acids were resolved in agarose gels. bp: base pairs.

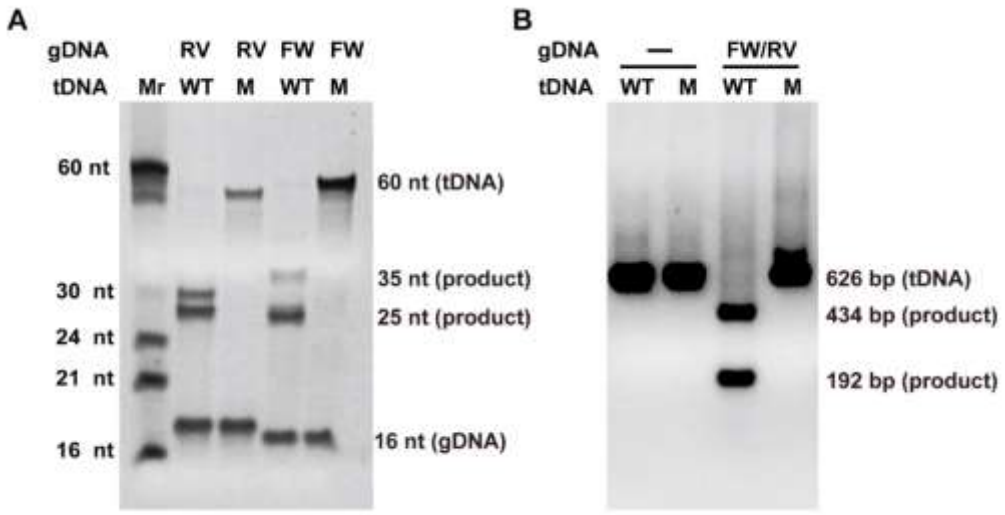

Figure S12. Cleavage discrimination of an *EGFR* del target directed by gDNA completely matching the WT sequence. **(A)** Cleavage efficiency for an *EGFR* del ssDNA target with a gDNA complementary to *EGFR* WT. **(B)** Cleavage efficiency for an *EGFR* del dsDNA target with a pair of gDNAs that completely paired with each strand of the WT dsDNA. *Pf*Ago loaded with the 16 nt gDNAs was incubated with the corresponding DNA target in a 1:10:1 molar ratio (*Pf*Ago: gDNA: tDNA) at 95 °C for 15 min. Nucleic acids were resolved in denaturing polyacrylamide gels **(A)** and agarose gels **(B)**. Mr: ssDNA marker; M: mutant ssDNA or dsDNA target; nt: nucleotides; bp: base pairs.

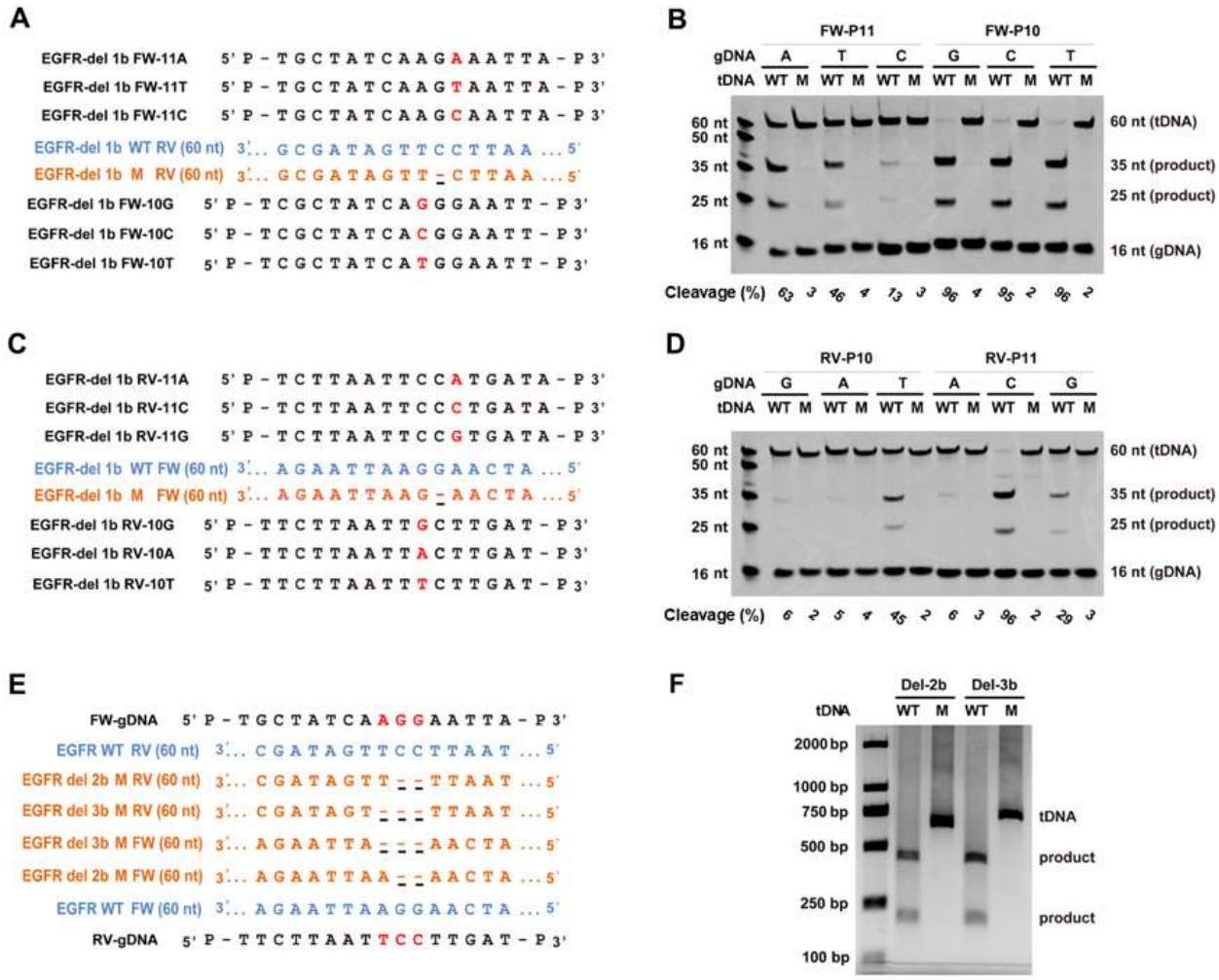

Figure S13. Cleavage discrimination of the synthetic *EGFR* deletion (1–3 bp) target directed by designed gDNA. **(A)** and **(C)** show the design of the gDNAs with different nucleotide substitutions at position 10 or 11 for both strands of the ssDNA targets. Mismatches are shown in red with the positions indicated. **(B)** and **(D)** show the results of gel electrophoresis of cleavage products for each strand of the ssDNA targets. **(E)** and **(F)** show the design of the gDNAs of *EGFR* deletion (2–3 bp) targets and the cleavage products for dsDNA targets. *Pf*Ago was incubated with 16 nt gDNAs, the WT and SNV ssDNA or dsDNA targets in a 1:10:1 molar ratio (*Pf*Ago: gDNA: tDNA) at 95 °C for 15 min. The cleavage products were resolved in denaturing polyacrylamide gels **(B, D)** and agarose gels **(F)**. M: SNV ssDNA or dsDNA target; nt: nucleotides; bp: base pairs.

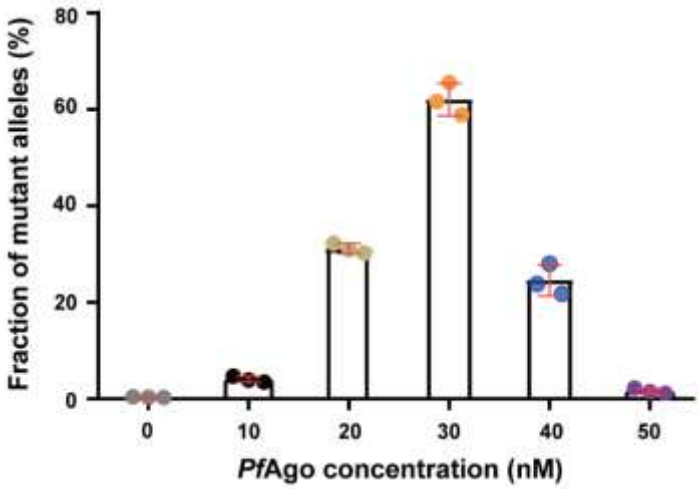

Figure S14. Effect of the *Pf*Ago concentration on A-Star enrichment for a 1% VAF of *KRAS* G12D. The *KRAS* G12D dsDNA target at a 1% VAF and 10 nM was tested with different *Pf*Ago concentrations but a consistent ratio of *Pf*Ago:gDNA (1:10) in the reactions. The enriched products were quantitatively measured using TaqMan qRT-PCR. Error bars represent the mean ± s.d., n = 3.

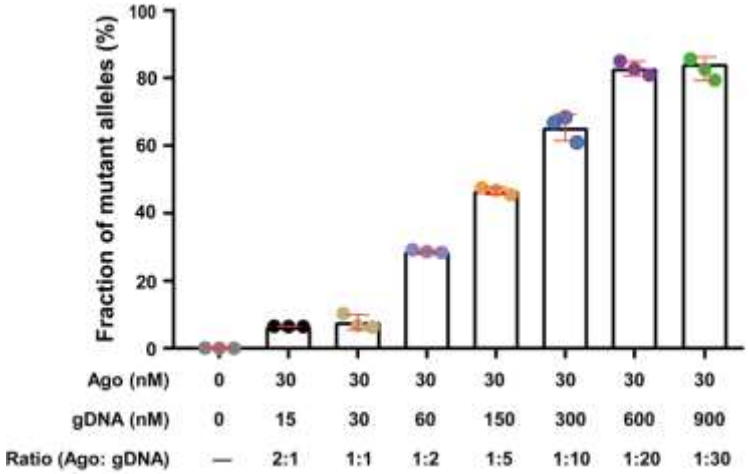

Figure S15. Effect of the ratio of *Pf*Ago:gDNA on A-Star enrichment for a 1% VAF of *KRAS* G12D. The dsDNA target with a 1% VAF of *KRAS* G12D at 10 nM was tested with different ratios of *Pf*Ago:gDNA but with a consistent 30 nM *Pf*Ago concentration in the reactions. The enriched samples were quantitatively measured using TaqMan qRT-PCR. Error bars represent the mean ± s.d., n = 3.

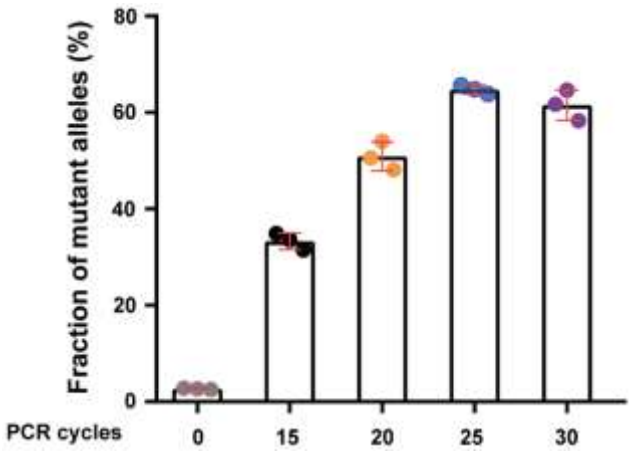

Figure S16. Effect of the PCR program on A-Star enrichment for a 1% VAF of *KRAS* G12D. The dsDNA target with a 1% VAF of *KRAS* G12D at 10 nM was tested using 30 nM *Pf*Ago and the *Pf*Ago:gDNA molar ratio was set to 1:20 in the reactions. Thermal cycling started with a preincubation step at 94 ℃ for 3 mins for polymerase activation and *Pf*Ago cleavage, followed by 15-30 PCR cycles (94 ℃ for 30 s, 55 ℃ for 30 s, and 72 ℃ for 20 s). The enriched products were quantitatively measured using TaqMan qRT-PCR. Error bars represent the mean ± s.d., n = 3.

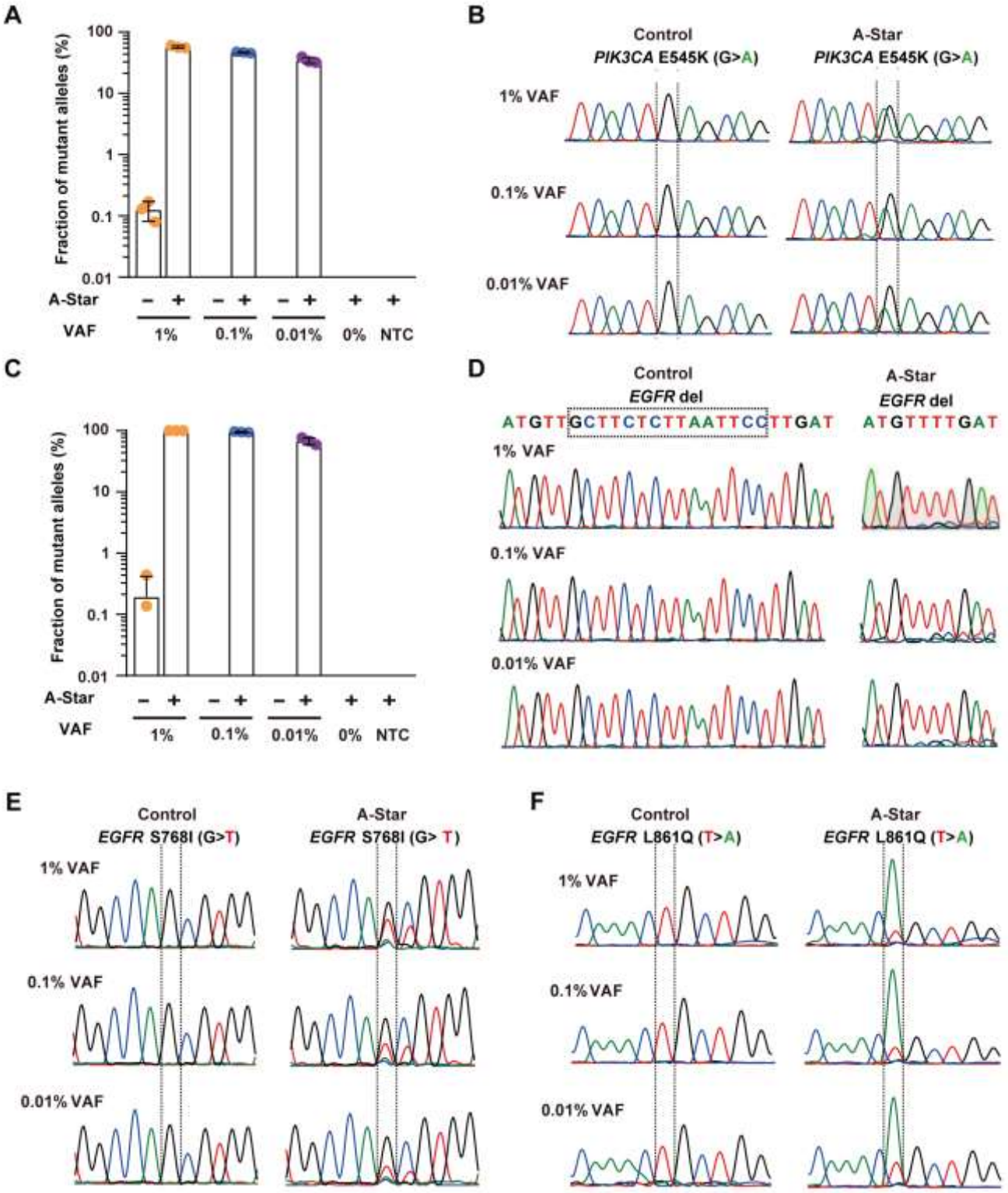

Figure S17. Evaluation of the A-Star enrichment results for samples with varying VAFs analyzed by TaqMan qRT-PCR and Sanger sequencing, including oncogenes of *PIK3CA* E545K **(A, B)**, *EGFR* del **(C, D)**, *EGFR* S768I **(E)** and *EGFR* L861Q **(F)**. Due to the lack of proper TaqMan probes for *EGFR* S768I and L861Q, the enriched products of the two oncogenes were detected using Sanger sequencing. All controls were performed in the absence of a pair of gDNAs. NTC contained only water. Error bars represent standard deviations of the mean, n = 3.

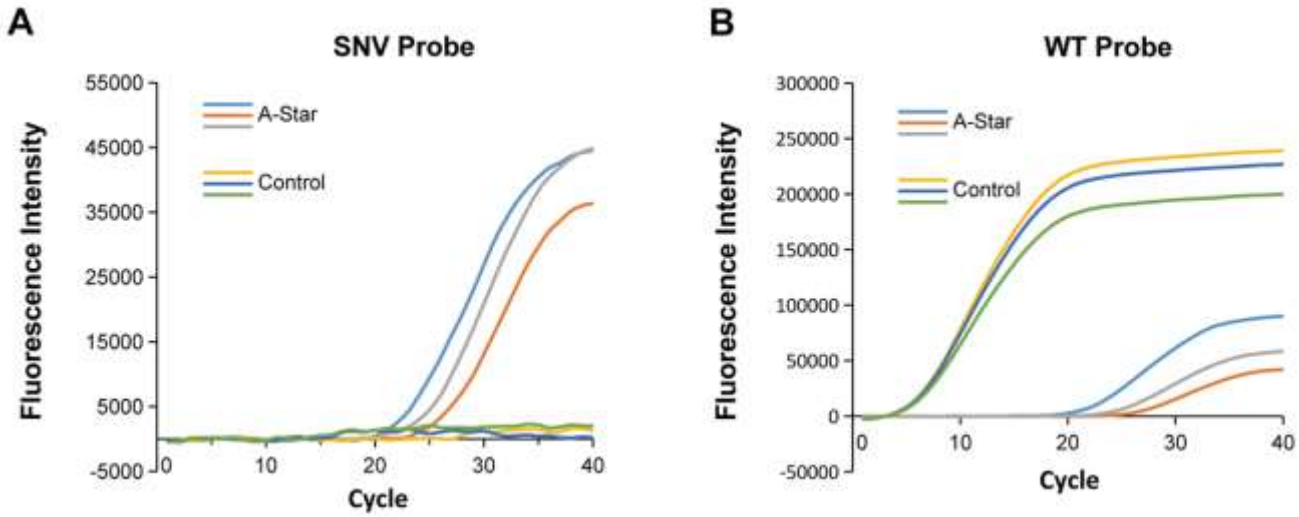

Figure S18. A strategy combining serial PCR reactions produced using the A-Star and Taqman qRT-PCR methods into a single PCR reaction for the detection of a 1% VAF of *KRAS* G12D. TaqMan qRT-PCR amplification curves with a specific probe for the WT **(A)** and SNV **(B)** targets. The template was 1 nM of the *KRAS* G12D sample with the 1% VAF of *KRAS* G12D. Template was then treated with either the two-step process of A-Star followed by Taqman qRT-PCR, or the single PCR reaction of combined A-Star and Taqman qRT-PCR. Each curve represents an independent repeat.

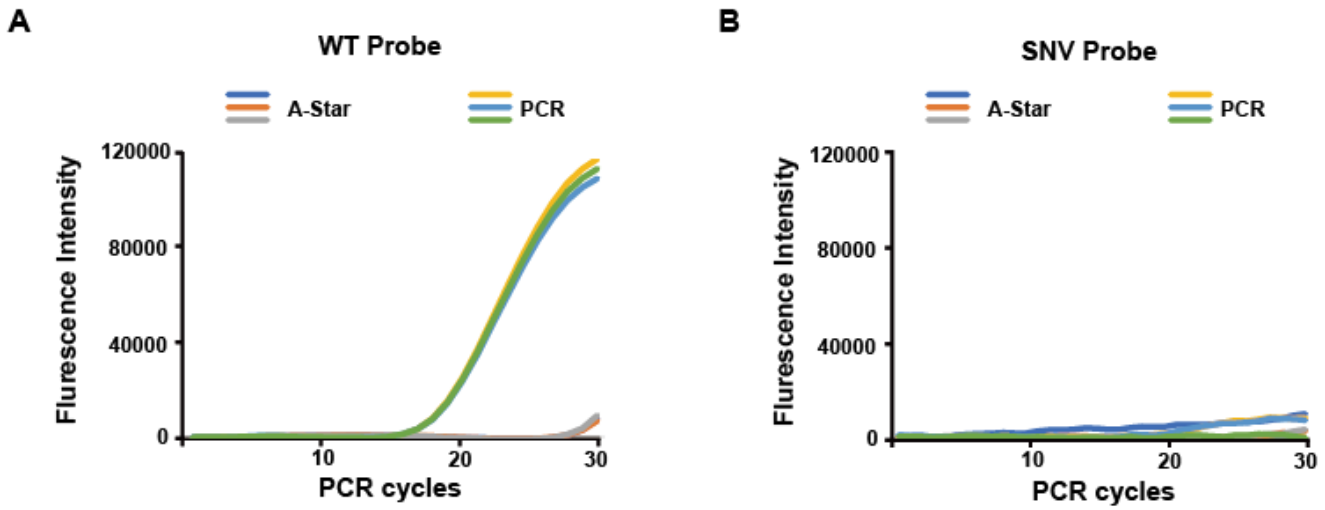

Figure S19. Comparison of amplification results for A-Star and routine PCR for a 1% VAF of *KRAS* G12D mock cfDNA standard. TaqMan qRT-PCR amplification curves with a specific probe for the WT **(A)** and an SNV **(B)** targets. The template was 33 ng Horizon cfDNA standard sample with 1% VAF of *KRAS* G12D and then used for treatment with either optimized A-Star or the routine PCR reaction. The amplicons were diluted 1,000-fold and then determined by TaqMan qRT-PCR. Each curve represents an independent repeat.

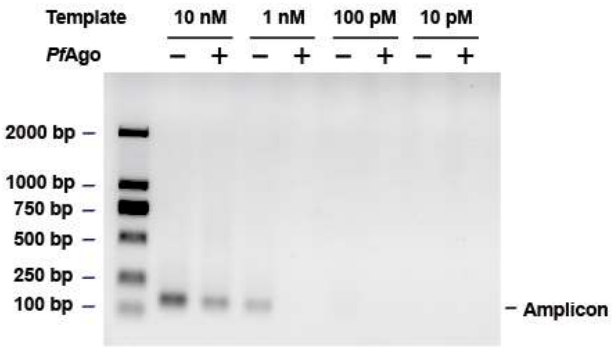

Figure S20. Evaluation of the binding phenomenon of *Pf*Ago when coupled with PCR. Various amounts (10 pM, 100 pM, 1 nM, and 10 nM) of the template were PCR amplified in absence or presence of 30 nM *Pf*Ago. The amplicons were analyzed by gel electrophoresis.

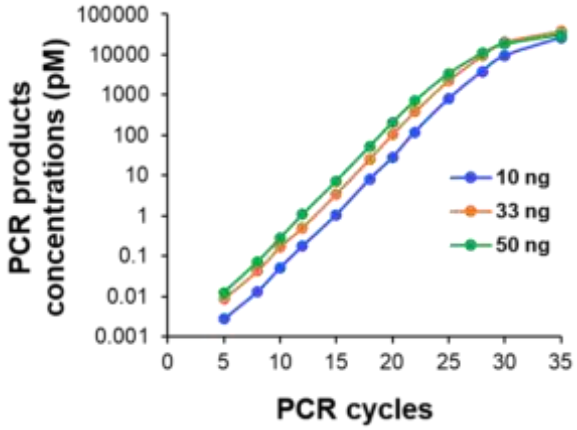

Figure S21. Product concentrations of PCR reactions with varied concentrations of *KRAS* G12D and different preamplification cycles. For the preamplification step, a high-fidelity enzyme (2X PCR Precision^{TM} MasterMix) was used and templates were from a 1% VAF of *KRAS* G12D mock cfDNA standard of varied concentrations (10 ng, 33 ng, and 50 ng). After PCR processed under evaluated cycles, the amplicons were quantitively determined by TaqMan qRT-PCR.

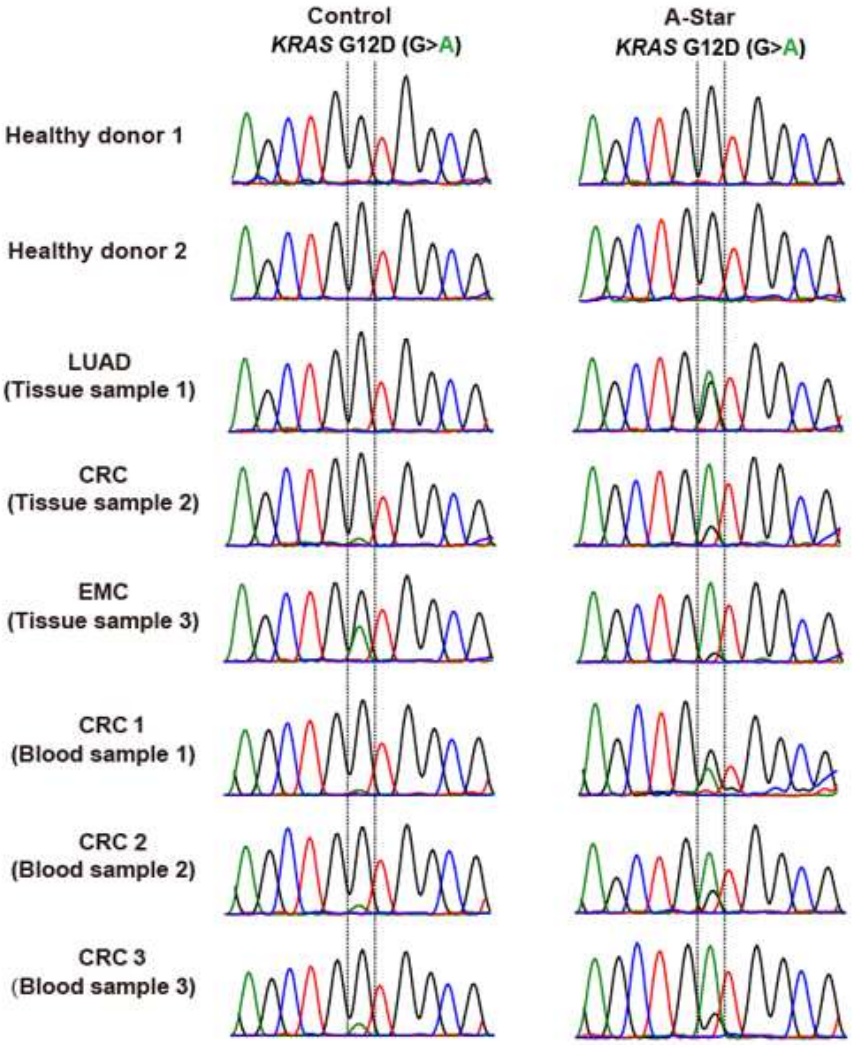

Figure S22. Evaluation of the A-Star enrichment results for clinical samples of diverse cancer types by Sanger sequencing. The clinical sample DNA was extracted and used as the input for A-Star, followed by analysis using Sanger sequencing. All controls were preprocessed in the absence of a pair of gDNAs. The original VAF of these clinically cancer samples are 0.03% (LUAD), 5.15% (CRC), 31.37% (EMC), 3.00% (CRC1), 4.74% (CRC2), 20.84% (CRC3), respectively.

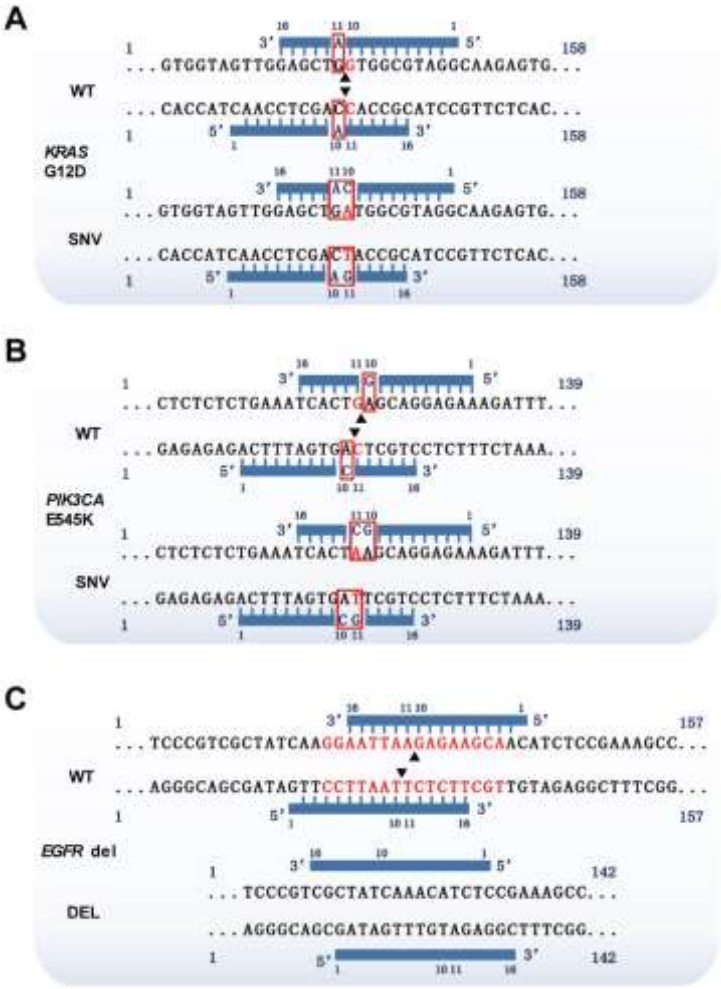

Figure S23. Diagram of the target region and gDNA design for the multiplex detection of *KRAS* G12D, *PIK3CA* E545K, and *EGFR* del. Mutations in the target are indicated in red; the mismatches introduced into the gDNAs are shown in red boxes; and the nucleotides deleted in *EGFR* del are highlighted in red.

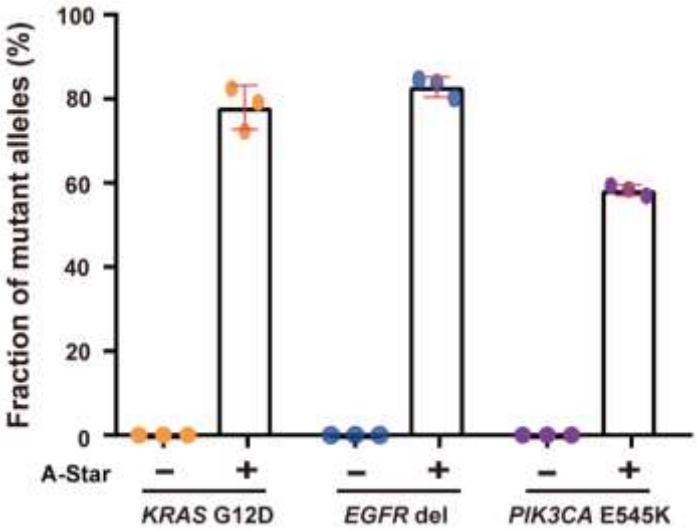

Figure S24. Evaluation of the A-Star multiplexed enrichment results for *KRAS* G12D, *PIK3CA* E545K, and *EGFR* del with the 1% VAF sample. The synthetic sample was mixed with a 1% VAF of *KRAS* G12D, *PIK3CA* E545K, and *EGFR* del at a 10 nM concentration and then used as the input for A-Star, followed by analysis with a TaqMan probe. All controls were preprocessed in the absence of a pair of gDNAs. Error bars represent the mean ± s.d., n = 3.

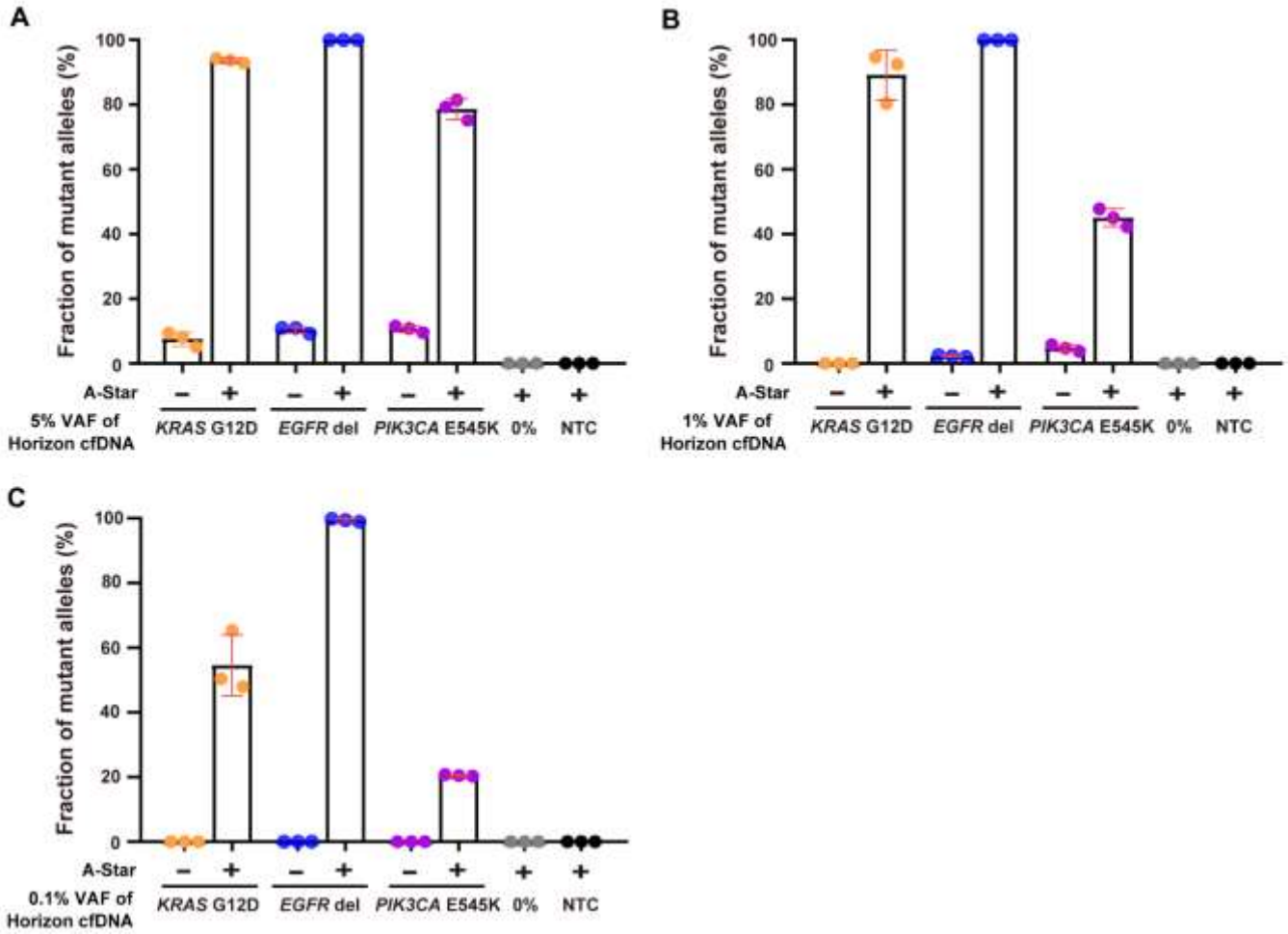

Figure S25. Evaluation of the A-Star triplex enrichment results for *KRAS* G12D, *PIK3CA* E545K, and *EGFR* del Horizon cfDNA standard samples with different VAFs of 5% **(A)**, 1% **(B)**, and 0.1% **(C)**. The standards were purchased from a commercial vendor (Horizon Discovery Group) and had different VAFs of 0.1%, 1%, and 5% for *KRAS* G12D, *PIK3CA* E545K, and *EGFR* del, respectively. A total of 33 ng/µl of these standards was used as the input to A-Star, followed by analysis via TaqMan qRT-PCR. All the controls were preprocessed in the absence of pairs of gDNAs. Error bars represent the mean ± s.d., n = 3.

Supplementary Table 1: Gene mutation for cancer types.

No.	Gene mutation	Cancer types
1	*KRAS* G12D	Colon cancer, Colorectal cancer, Hairy cell leukemia, Lung cancer, Non-small cell lung cancer, Melanoma, Multiple myeloma, Ovarian cancer, Pancreatic ductal cancer, Cutaneous squamous cell carcinoma, Thyroid carcinoma, Exocrine pancreatic tumor
2	*EGFR* L861Q	Non-small cell lung cancer, Malignant glioma
3	*EGFR* S768I	Lung adenocarcinoma, Non-small cell lung cancer
4	*EGFR del* E746-A750	Non-small cell lung cancer, Lung adenocarcinoma
5	*PIK3CA* E545K	Breast cancer, Cervical cancer, Colorectal cancer, Lung adenocarcinoma, Non-small cell lung cancer, Melanoma

Supplementary Table 2: gDNAs used in this study.

Name	gDNA sequence (5'→3')	Target	Presence
KRAS- FW	P-TTTGGAGCTGGTGGCG	*KRAS*-(WT)-RV/*KRAS*-(M)-RV	Fig. S1
KRAS- RV	P-TCCTACGCCACCAGCT	*KRAS*-(WT)-WT/*KRAS*-(M)-WT	Fig. S4
*KRAS*_gM3	P-TTAGGAGCTGGTGGCG-P	*KRAS*-(WT)-RV/*KRAS*-(M)-RV	Fig. 2/Fig. S5
*KRAS*_gM4	P-TTTCGAGCTGGTGGCG-P	*KRAS*-(WT)-RV/*KRAS*-(M)-RV	Fig. 2/Fig. S5
*KRAS*_gM5	P-TTTGCAGCTGGTGGCG-P	*KRAS*-(WT)-RV/*KRAS*-(M)-RV	Fig. 2/Fig. S5
*KRAS*_gM6	P-TTTGGTGCTGGTGGCG-P	*KRAS*-(WT)-RV/*KRAS*-(M)-RV	Fig. 2/Fig. S5
*KRAS*_gM7	P-TTTGGACCTGGTGGCG-P	*KRAS*-(WT)-RV/*KRAS*-(M)-RV	Fig. 2/Fig. S5
*KRAS*_gM8	P-TTTGGAGGTGGTGGCG-P	*KRAS*-(WT)-RV/*KRAS*-(M)-RV	Fig. 2/Fig. S5
*KRAS*_gM9	P-TTTGGAGCAGGTGGCG-P	*KRAS*-(WT)-RV/*KRAS*-(M)-RV	Fig. 2/Fig. S5
*KRAS*_gM10	P-TTTGGAGCTAGTGGCG-P	*KRAS*-(WT)-RV/*KRAS*-(M)-RV	Fig. 2/Fig. S5
*KRAS*_gM11	P-TCTACGCCACGAGCTC-P	*KRAS*-(WT)-FW/*KRAS*-(M)-FW	Fig. 2/Fig. S5
KRAS-G12D RV-10T	P-TCCTACGCCTCCAGCT-P	*KRAS*-(WT)-FW/*KRAS*-G12A/V/D-(M)-FW	Fig. S7
KRAS-G12D RV-10G	P-TCCTACGCCGCCAGCT-P	*KRAS*-(WT)-FW/*KRAS*-G12A/V/D- (M)-FW	Fig. S7
KRAS-G12D RV-10C	P-TCCTACGCCCCCAGCT-P	*KRAS*-(WT)-FW/*KRAS*- G12A/V/D-(M)-FW	Fig. S7
KRAS-G12D RV-11A	P-TCTACGCCACAAGCTC-P	*KRAS*-(WT)-FW/*KRAS*- G12A/V/D-(M)-FW	Fig. 2-6 /Fig. S7, S11, S14-19, S22-25
KRAS-G12D RV-11T	P-TCTACGCCACTAGCTC-P	*KRAS*-(WT)-FW/*KRAS*- G12A/V/D-(M)-FW	Fig. S7
KRAS-G12D RV-11G	P-TCTACGCCACGAGCTC-P	*KRAS*-(WT)-FW/*KRAS*- G12A/V/D-(M)-FW	Fig. S7
KRAS-G12D FW-10A	P-TTTGGAGCTAGTGGCG-P	*KRAS*-(WT)-RV/*KRAS*- G12A/V/D-(M)-RV	Fig. 2-6 /Fig. S7, S11, S14-19, S22-25
KRAS-G12D FW-10T	P-TTTGGAGCTTGTGGCG-P	*KRAS*-(WT)-RV/*KRAS*- G12A/V/D-(M)-RV	Fig. S7
KRAS-G12D FW-10C	P-TTTGGAGCTCGTGGCG-P	*KRAS*-(WT)-RV/*KRAS*- G12A/V/D-(M)-RV	Fig. S7
KRAS-G12D FW-11A	P-TTGGAGCTGGAGGCGT-P	*KRAS*-(WT)-RV/*KRAS*- G12A/V/D-(M)-RV	Fig. S7
KRAS-G12D FW-11G	P-TTGGAGCTGGGGGCGT-P	*KRAS*-(WT)-RV/*KRAS*- G12A/V/D-(M)-RV	Fig. S7
KRAS-G12D FW-11C	P-TTGGAGCTGGCGGCGT-P	*KRAS*-(WT)-RV/*KRAS*- G12A/V/D-(M)-RV	Fig. S7
*PIK3CA*_gM2	P-TCAAATCACTGAGCAG-P	*PIK3CA*-(WT)-RV/*PIK3CA*-(M)-RV	Fig. S6
*PIK3CA*_gM3	P-TGTAATCACTGAGCAG-P	*PIK3CA*-(WT)-RV/*PIK3CA*-(M)-RV	Fig. S6
*PIK3CA*_gM4	P-TGATATCACTGAGCAG-P	*PIK3CA*-(WT)-RV/*PIK3CA*-(M)-RV	Fig. S6
*PIK3CA*_gM5	P-TGAATTCACTGAGCAG-P	*PIK3CA*-(WT)-RV/*PIK3CA*-(M)-RV	Fig. S6
*PIK3CA*_gM6	P-TGAAAACACTGAGCAG-P	*PIK3CA*-(WT)-RV/*PIK3CA*-(M)-RV	Fig. S6
*PIK3CA*_gM7	P-TGAAATGACTGAGCAG-P	*PIK3CA*-(WT)-RV/*PIK3CA*-(M)-RV	Fig. S6
*PIK3CA*_gM8	P-TGAAATCTCTGAGCAG-P	*PIK3CA*-(WT)-RV/*PIK3CA*-(M)-RV	Fig. S6
*PIK3CA*_gM9	P-TGAAATCAGTGAGCA-P	*PIK3CA*-(WT)-RV/*PIK3CA*-(M)-RV	Fig. S6
*PIK3CA*_gM10	P-TGAAATCACAGAGCAG-P	*PIK3CA*-(WT)-RV/*PIK3CA*-(M)-RV	Fig. S6
*PIK3CA*_gM11	P-TGAAATCACAGAGCAG-P	*PIK3CA*-(WT)-RV/*PIK3CA*-(M)-RV	Fig. S6

PIK3CA-RV-10A	P-TTCTCCTGCACAGTGA-P	*PIK3CA*-(WT)-FW/*PIK3CA*-(M)-FW	Fig. S8
PIK3CA-RV-10G	P-TTCTCCTGCGCAGTGA-P	*PIK3CA*-(WT)-FW/*PIK3CA*-(M)-FW	Fig. 4, 6/Fig. S8, S17, S22-25
PIK3CA-RV-10C	P-TTCTCCTGCCCAGTGA-P	*PIK3CA*-(WT)-FW/*PIK3CA*-(M)-FW	Fig. S8
PIK3CA-RV-11T	P-TCTCCTGCTCTGTGAT-P	*PIK3CA*-(WT)-FW/*PIK3CA*-(M)-FW	Fig. S8
PIK3CA-RV-11G	P-TCTCCTGCTCGGTGAT-P	*PIK3CA*-(WT)-FW/*PIK3CA*-(M)-FW	Fig. S8
PIK3CA-RV-11C	P-TCTCCTGCTCCGTGAT-P	*PIK3CA*-(WT)-FW/*PIK3CA*-(M)-FW	Fig. S8
PIK3CA-FW-10A	P-TGAAATCACAGAGCAG-P	*PIK3CA*-(WT)-RV/*PIK3CA*-(M)-RV	Fig. S8
PIK3CA-FW-10G	P-TGAAATCACGGAGCAG-P	*PIK3CA*-(WT)-RV/*PIK3CA*-(M)-RV	Fig. S8
PIK3CA-FW-10C	P-TGAAATCACCGAGCAG-P	*PIK3CA*-(WT)-RV/*PIK3CA*-(M)-RV	Fig. 4, 6/Fig. S8, S17, S22-25
PIK3CA-FW-11T	P-TAAATCACTGTGCAGG-P	*PIK3CA*-(WT)-RV/*PIK3CA*-(M)-RV	Fig. S8
PIK3CA-FW-11G	P-TAAATCACTGGGCAGG-P	*PIK3CA*-(WT)-RV/*PIK3CA*-(M)-RV	Fig. S8
PIK3CA-FW-11C	P-TAAATCACTGCGCAGG-P	*PIK3CA*-(WT)-RV/*PIK3CA*-(M)-RV	Fig. S8
EGFR-RV (Del-di-P)	P-TTTGCTTCTCTTAATT-P	*EGFR*-(WT)-FW-Del/*EGFR*-(M)-FW-Del	Fig. 4, 6/Fig. S12, S17, S22-25
EGFR-FW (Del-di-P)	P-TAAGGAATTAAGAGAA-P	*EGFR*-(WT)-RV-Del/*EGFR*-(M)-RV-Del	Fig. 4, 6/Fig. S12, S17, S22-25
EGFR-del 1b RV-10G	P-TTCTTAATTGCTTGAT-P	*EGFR*-Del- (WT)- FW/*EGFR*-del 1b- (M)- FW	Fig. S13
EGFR-del 1b RV-10A	P-TTCTTAATTACTTGAT-P	*EGFR*-Del- (WT)- FW/*EGFR*-del 1b- (M)- FW	Fig. S13
EGFR-del 1b RV-10T	P-TTCTTAATTTCTTGAT-P	*EGFR*-Del- (WT)- FW/*EGFR*-del 1b- (M)- FW	Fig. S13
EGFR-del 1b RV-11A	P-TCTTAATTCCATGATA-P	*EGFR*-Del- (WT)- FW/*EGFR*-del 1b- (M)- FW	Fig. S13
EGFR-del 1b RV-11C	P-TCTTAATTCCCTGATA-P	*EGFR*-Del- (WT)- FW/*EGFR*-del 1b- (M)- FW	Fig. S13
EGFR-del 1b RV-11G	P-TCTTAATTCCGTGATA-P	*EGFR*-Del- (WT)- FW/*EGFR*-del 1b- (M)- FW	Fig. S13
EGFR-del 1b FW-11A	P-TGCTATCAAGAAATTA-P	*EGFR*-Del- (WT)- RV/*EGFR*-del 1b- (M)- RV	Fig. S13
EGFR-del 1b FW-11T	P-TGCTATCAAGTAATTA-P	*EGFR*-Del- (WT)- RV/*EGFR*-del 1b- (M)- RV	Fig. S13
EGFR-del 1b FW-11C	P-TGCTATCAAGCAATTA-P	*EGFR*-Del- (WT)- RV/*EGFR*-del 1b- (M)- RV	Fig. S13
EGFR-del 1b FW-10G	P-TCGCTATCAGGGAATT-P	*EGFR*-Del- (WT)- RV/*EGFR*-del 1b- (M)- RV	Fig. S13
EGFR-del 1b FW-10C	P-TCGCTATCACGGAATT-P	*EGFR*-Del- (WT)- RV/*EGFR*-del 1b- (M)- RV	Fig. S13
EGFR-del 1b FW-10T	P-TCGCTATCATGGAATT-P	*EGFR*-Del- (WT)- RV/*EGFR*-del 1b- (M)- RV	Fig. S13
EGFR-del 2b RV	P-TTCTTAATTCCTTGAT-P	*EGFR*-Del- (WT)- FW/ *EGFR*-del 2b- (M)- FW	Fig. S13
EGFR-del 2b FW	P-TGCTATCAAGGAATTA-P	*EGFR*-Del- (WT)- RV/ *EGFR*-del 2b- (M)- RV	Fig. S13
EGFR L861Q-RV-10T	P-TGCACCCAGTAGTTTG-P	*EGFR* L861Q-(WT)-FW/*EGFR* L861Q-(M)-FW	Fig. S9
EGFR L861Q-RV-10A	P-TGCACCCAGAAGTTTG-P	*EGFR* L861Q-(WT)-FW/*EGFR* L861Q-(M)-FW	Fig. S9
EGFR L861Q-RV-10G	P-TGCACCCAGGAGTTTG-P	*EGFR* L861Q-(WT)-FW/*EGFR* L861Q-(M)-FW	Fig. S9
EGFR L861Q-RV-11T	P-TCACCCAGCATTTTGG-P	*EGFR* L861Q-(WT)-FW/*EGFR* L861Q-(M)-FW	Fig. S9
EGFR L861Q-RV-11A	P-TCACCCAGCAATTTGG-P	*EGFR* L861Q-(WT)-FW/*EGFR* L861Q-(M)-FW	Fig. S9, S17
EGFR L861Q-RV-11C	P-TCACCCAGCACTTTGG-P	*EGFR* L861Q-(WT)-FW/*EGFR* L861Q-(M)-FW	Fig. S9
EGFR L861Q-FW-10G	P-TTGGCCAAAGTGCTGG-P	*EGFR* L861Q-(WT)-FW/*EGFR* L861Q-(M)-FW	Fig. S9, S17
EGFR L861Q-FW-10A	P-TTGGCCAAAATGCTGG-P	*EGFR* L861Q-(WT)-FW/*EGFR* L861Q-(M)-FW	Fig. S9

EGFR L861Q-FW-10T	P-TTGGCCAAATTGCTGG-P	*EGFR* L861Q-(WT)-FW/*EGFR* L861Q-(M)-FW	Fig. S9
EGFR L861Q-FW-11C	P-TGGCCAAACTCCTGGG-P	*EGFR* L861Q-(WT)-FW/*EGFR* L861Q-(M)-FW	Fig. S9
EGFR L861Q-FW-11A	P-TGGCCAAACTACTGGG-P	*EGFR* L861Q-(WT)-FW/*EGFR* L861Q-(M)-FW	Fig. S9
EGFR L861Q-FW-11T	P-TGGCCAAACTTCTGGG-P	*EGFR* L861Q-(WT)-FW/*EGFR* L861Q-(M)-FW	Fig. S9
EGFR S768I-RV-10C	P-TTTGTCCACCCTGGCC-P	*EGFR* S768I-(WT)-FW/*EGFR* S768I-(M)-FW	Fig. S10
EGFR S768I-RV-10A	P-TTTGTCCACACTGGCC-P	*EGFR* S768I-(WT)-FW/*EGFR* S768I-(M)-FW	Fig. S10
EGFR S768I-RV-10T	P-TTTGTCCACTCTGGCC-P	*EGFR* S768I-(WT)-FW/*EGFR* S768I-(M)-FW	Fig. S10, S17
EGFR S768I-RV-11A	P-TTGTCCACGCAGGCCA-P	*EGFR* S768I-(WT)-FW/*EGFR* S768I-(M)-FW	Fig. S10
EGFR S768I-RV-11G	P-TTGTCCACGCGGGCCA-P	*EGFR* S768I-(WT)-FW/*EGFR* S768I-(M)-FW	Fig. S10
EGFR S768I-RV-11C	P-TTGTCCACGCCGGCCA-P	*EGFR* S768I-(WT)-FW/*EGFR* S768I-(M)-FW	Fig. S10
EGFR S768I-FW-10T	P-TTGATGGCCTGCGTGG-P	*EGFR* S768I-(WT)-RV/*EGFR* S768I-(M)-RV	Fig. S10, S17
EGFR S768I-FW-10G	P-TTGATGGCCGGCGTGG-P	*EGFR* S768I-(WT)-RV/*EGFR* S768I-(M)-RV	Fig. S10
EGFR S768I-FW-10C	P-TTGATGGCCCGCGTGG-P	*EGFR* S768I-(WT)-RV/*EGFR* S768I-(M)-RV	Fig. S11
EGFR S768I-FW-11G	P-TGATGGCCAGGGTGGA-P	*EGFR* S768I-(WT)-RV/*EGFR* S768I-(M)-RV	Fig. S10
EGFR S768I-FW-11A	P-TGATGGCCAGAGTGGA-P	*EGFR* S768I-(WT)-RV/*EGFR* S768I-(M)-RV	Fig. S10
EGFR S768I-FW-11T	P-TGATGGCCAGTGTGGA-P	*EGFR* S768I-(WT)-RV/*EGFR* S768I-(M)-RV	Fig. S10
15 nt gDNA	P-CATTTGGGCGTGCCC	ssDNA F-Q substrate	Fig. S2
20 nt gDNA	P-CATTTGGGCGTGCCCC CGCA	ssDNA F-Q substrate	Fig. S2
25 nt gDNA	P-CATTTGGGCGTGCCCC CGCAAGACT	ssDNA F-Q substrate	Fig. S2
30 nt gDNA	P-CATTTGGGCGTGCCCC CGCAAGACTGCTAG	ssDNA F-Q substrate	Fig. S2
40 nt gDNA	P-CATTTGGGCGTGCCCC CGCAAGACTGCTAGCCG AGTAGCG	ssDNA F-Q substrate	Fig. S2
50 nt gDNA	P-CATTTGGGCGTGCCCC CGCAAGACTGCTAGCCG AGTAGCGTTGGGTTGCG	ssDNA F-Q substrate	Fig. S2
60 nt gDNA	P-CATTTGGGCGTGCCCC CGCAAGACTGCTAGCCG AGTAGCGTTGGGTTGCG AAAGGCCTTG	ssDNA F-Q substrate	Fig. S2
70 nt gDNA	P-CATTTGGGCGTGCCCC CGCAAGACTGCTAGCCG AGTAGCGTTGGGTTGCG AAAGGCCTTGTGGTACT GCC	ssDNA F-Q substrate	Fig. S2
80 nt gDNA	P-CATTTGGGCGTGCCCC CGCAAGACTGCTAGCCG AGTAGCGTTGGGTTGCG AAAGGCCTTGTGGTACT GCCTGATAGGGCG	ssDNA F-Q substrate	Fig. S2

Supplementary Table 3: ssDNA targets used in this study.

Name	Sequence (5'→3')	Presence
KRAS-(WT)- FW	TATAAACTTGTGGTAGTTGGAGCTGGTGGC GTAGGCAAGAGTGCCTTGACGATACAGCTA	Fig.2/Fig. S7
KRAS- (WT)- RV	TAGCTGTATCGTCAAGGCACTCTTGCCTAC GCCACCAGCTCCAACTACCACAAGTTTATA	Fig. 2/Fig. S1, S4-S5, S7
KRAS-G12D-(M)- FW	TATAAACTTGTGGTAGTTGGAGCTGATGGC GTAGGCAAGAGTGCCTTGACGATACAGCTA	Fig. 2/Fig. S7
KRAS-G12D-(M)- RV	TAGCTGTATCGTCAAGGCACTCTTGCCTAC GCCATCAGCTCCAACTACCACAAGTTTATA	Fig. 2/Fig. S4-S5, S7
PIK3CA-(WT)-FW	AATTTCTACACGAGATCCTCTCTCTGAAATC ACTGAGCAGGAGAAAGATTTTCTATGGAG	Fig. S6, S8
PIK3CA-(WT)-RV	CTCCATAGAAAATCTTTCTCCTGCTCAGTGA TTTCAGAGAGAGGATCTCGTGTAGAAATT	Fig. S6, S8
PIK3CA-(M)-FW	AATTTCTACACGAGATCCTCTCTCTGAAATC ACTAAGCAGGAGAAAGATTTTCTATGGAG	Fig. S6, S8
PIK3CA-(M)-RV	CTCCATAGAAAATCTTTCTCCTGCTTAGTGA TTTCAGAGAGAGGATCTCGTGTAGAAATT	Fig. S6, S8
EGFR-(WT)-FW-Del	AAAATTCCCGTCGCTATCAAGGAATTAAGA GAAGCAACATCTCCGAAAGCCAACAAGGAA	Fig. S12
EGFR-(WT)-RV-Del	TTCCTTGTTGGCTTTCGGAGATGTTGCTTC TCTTAATTCCTTGATAGCGACGGGAATTTT	Fig. S12
EGFR-(M)-FW-Del	AAAGTTAAAATTCCCGTCGCTATCAAAACA TCTCCGAAAGCCAACAAGGAAATCCTCGAT	Fig. S12
EGFR-(M)-RV-Del	ATCGAGGATTTCCTTGTTGGCTTTCGGAGA TGTTTTGATAGCGACGGGAATTTTAACTTT	Fig. S12
EGFR-Del- (WT)- RV	TTGTTGGCTTTCGGAGATGTTGCTTCTCTT AATTCCTTGATAGCGACGGGAATTTTAACT	Fig. S13
EGFR-Del- (WT)- FW	AGTTAAAATTCCCGTCGCTATCAAGGAATT AAGAGAAGCAACATCTCCGAAAGCCAACAA	Fig. S13
EGFR-del 1b- (M)- RV	TTGTTGGCTTTCGGAGATGTTGCTTCTCTT AATTCTTGATAGCGACGGGAATTTTAACT	Fig. S13
EGFR-del 1b- (M)- FW	AGTTAAAATTCCCGTCGCTATCAAGAATT AAGAGAAGCAACATCTCCGAAAGCCAACAA	Fig. S13
EGFR L861Q-(WT)-FW	ATCACAGATTTTGGGCTGGCCAAACTGCTG GGTGCGGAAGAGAAAGAATACCATGCAGAA	Fig. S9
EGFR L861Q-(M)-FW	ATCACAGATTTTGGGCTGGCCAAACAGCTG GGTGCGGAAGAGAAAGAATACCATGCAGAA	Fig. S9
EGFR L861Q-(WT)-RV	TTCTGCATGGTATTCTTTCTCTTCCGCACC CAGCAGTTTGGCCAGCCCAAAATCTGTGAT	Fig. S9
EGFR L861Q-(M)-RV	TTCTGCATGGTATTCTTTCTCTTCCGCACC CAGCTGTTTGGCCAGCCCAAAATCTGTGAT	Fig. S9

EGFR S768I-(WT)-FW	CTCCAGGAAGCCTACGTGATGGCCAGCGTG GACAACCCCCACGTGTGCCGCCTGCTGGGC	Fig. S10
EGFR S768I-(M)-FW	CTCCAGGAAGCCTACGTGATGGCCATCGTG GACAACCCCCACGTGTGCCGCCTGCTGGGC	Fig. S10
EGFR S768I-(WT)-RV	GCCCAGCAGGCGGCACACGTGGGGGTTGTC CACGCTGGCCATCACGTAGGCTTCCTGGAG	Fig. S10
EGFR S768I-(M)-RV	GCCCAGCAGGCGGCACACGTGGGGGTTGTC CACGATGGCCATCACGTAGGCTTCCTGGAG	Fig. S10
ssDNA F-Q substrate	FAM-CTCGGCTAGCAGTCTTGCGGGGGCAC GCCCAAATGGCCGG-BHQ1	Fig. S2

Supplementary Table 4: Primers used in this study.

Name	Target	Primer sequence (5'→3')	Presence
KRAS-158FW	*KRAS* (G12D)	GTGACATGTTCTAATATAGTC	Fig. 2-6/Fig. S14-S16, S18-S22, S24, S25
KRAS-158RV	*KRAS* (G12D)	GGATCATATTCGTCCACAAA	Fig. 2-6/Fig. S14-S16, S18-S22, S24, S25
PIK3CA-139FW	*PIK3CA* (E545K)	GAGACAATGAATTAAGGGAA	Fig. 4, 6/Fig. S17, S24, S25
PIK3CA-139RV	*PIK3CA* (E545K)	GAAACAGAGAATCTCCATT	Fig. 4, 6/Fig. S17, S24, S25
EGFR-157FW	*EGFR* (delE746-A750)	CTGTCATAGGGACTCTGGAT	Fig. 4, 6/Fig. S17, S24, S25
EGFR-157RV	*EGFR* (delE746-A750)	GCCTGAGGTTCAGAGCCAT	Fig. 4, 6/Fig. S17, S24, S25
EGFR S768I-158FW	*EGFR* (S768I)	GCGAAGCCACACTGAC	Fig. S17
EGFR S768I-158RV	*EGFR* (S768I)	GACGGAGGACCTGATACA	Fig. S17
EGFR L861Q-147FW	*EGFR* (L861Q)	GAGGACCGTCGCTTGGT	Fig. S17
EGFR L861Q-147RV	*EGFR* (L861Q)	GTCTTCCTCCGTTTCATTCC	Fig. S17
M13F (-47)	~600 bp dsDNA target	CGCCAGGGTTTTCCCAGTCACGAC	Fig. 2/Fig. S3, S7-S13
M13R (-48)	~600 bp dsDNA target	AGCGGATAACAATTTCACACAGGA	Fig. 2/Fig. S3, S7-S13

Supplementary Table 5: TaqMan probes and primers used in this study.

Name	Sequence (5'-3')
PIK3CA-Forward Primer	5’-GAACAGCTCAAAGCAATTTCTACAC-3’
PIK3CA-Reverse Primer	5’-AGCACTTACCTGTGACTCCATAG-3’
PIK3CA (wt)-TaqMan Probe	5’- CTGAAATCACTGAGCAGGA-3’ (FAM-BHQ1)
PIK3CA E545K-TaqMan Probe	5’- TCTGAAATCACTAAGCAGGA-3’(VIC-BHQ1)
KRAS-Forward Primer	5’-AGGCCTGCTGAAAATGACTG-3’
KRAS-Reverse Primer	5’-GCTGTATCGTCAAGGCACTCT-3’
KRAS (wt)-TaqMan Probe	5’-TTGGAGCTGGTGGCGTA-3’(VIC-BHQ1)
KRAS G12D-TaqMan Probe	5’-TTGGAGCTGATGGCGTA-3’(FAM-BHQ1)
EGFR-Forward Primer	5’- CCAGAAGGTGAGAAAGTTA-3’
EGFR-Reverse Primer	5’-TCGAGGATTTCCTTGTTG-3’
EGFR (wt)-TaqMan Probe	5’-CTTCTCTTAATTCCTTGATAGCGACGG-3’(FAM-BHQ1)
EGFR del E746-A750-TaqMan Probe	5’-CGCTATCAAAACATCTCCGAAAGCC-3’(VIC-BHQ1)

Supplementary Table 6: Clinical samples used in this study.

Patient number	Cancer types	Genotype and mutation fraction*	Presence
Tissue sample 1	Lung adenocarcinoma	*KRAS* G12D	Fig. 5/Fig. S22
Tissue sample 2	Colorectal cancer	*KRAS* G12D	Fig. 5/Fig. S22
Tissue sample 3	Endometrial cancer	*KRAS* G12D	Fig. 5/Fig. S22
Blood sample 1	Colorectal cancer	*KRAS* G12D	Fig. 5/Fig. S22
Blood sample 2	Colorectal cancer	*KRAS* G12D	Fig. 5/Fig. S22
Blood sample 3	Colorectal cancer	*KRAS* G12D	Fig. 5/Fig. S22
Healthy donor 1	ND**	—	Fig. 5/Fig. S22
Healthy donor 1	ND**	—	Fig. 5/Fig. S22

*Samples were analyzed with standard NGS protocol; **Not detected, possibly because the mutant allele was not present.